INTERNATIONAL JOURNAL OF HYDROGEN ENERGY XXX (XXXX) XXX

Available online at www.sciencedirect.com

ScienceDirect

journal homepage: www.elsevier.com/locate/he

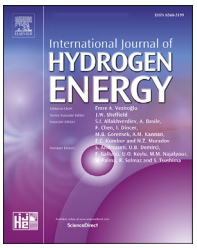

Effect of hydrogen direct injection on natural gas/hydrogen engine performance under high compression-ratio conditions

Lin Chen [a,*], *Xiao Zhang* [a], *Ren Zhang* [b], *Jinguang Li* [b], *Jiaying Pan* [b,**], *Haiqiao Wei* [b]

[a] *School of Optical Information and Energy Engineering, Wuhan Institute of Technology, Wuhan, 430205, PR China*
[b] *State Key Laboratory of Engines, Tianjin University, Tianjin, 300072, PR China*

HIGHLIGHTS

- Effect of hydrogen injection on methane combustion was optically studied.
- Hydrogen addition mainly acts as an ignition promoter for methane lean combustion.
- Suitable late injection can improve the natural gas/hydrogen engine's performance.
- Late hydrogen injection is more effective under lean conditions.

ARTICLE INFO

Article history:
Received 6 June 2022
Received in revised form
17 July 2022
Accepted 20 July 2022
Available online xxx

Keywords:
Natural gas
Hydrogen direct injection
Lean combustion
Optical engine
Flame propagation

ABSTRACT

In traffic transportation, the use of low-carbon fuels is the key to being carbon-neutral. Hydrogen-enhanced natural gas gets more and more attention, but practical engines fueled with it often suffer from low engine power output. In this study, the inner mechanism of hydrogen direct injection on methane combustion was optically studied based on a dual-fuel supply system. Simultaneous pressure acquisition and high-speed direct photography were used to analyze engine performance and flame characteristics. The results show that lean combustion can improve methane engine's thermal efficiency, but is limited by cyclic variations under high excess air coefficient conditions. Hydrogen addition mainly acts as an ignition promoter for methane lean combustion, as a result, the lean combustion limit and thermal efficiency can be improved. As for hydrogen injection timing, late injection can increase the in-cylinder turbulence intensity but also the inhomogeneity, so a suitable injection timing is needed for improving the engine's performance. Besides, late hydrogen injection is more effective under lean conditions because of the reduced mixture inhomogeneity. The current study shall give some insights into the controlling strategies for natural gas/hydrogen engines.

* *Corresponding author.*
** *Corresponding author.*
E-mail addresses: chenlin@wit.edu.cn (L. Chen), jypan@tju.edu.cn (J. Pan).

https://doi.org/10.1016/j.ijhydene.2022.07.176
0360-3199/

Nomenclature

NG	Natural gas
SI	Spark-ignition
HCNG	Hydrogen-enriched compression natural gas
RPM	Revolutions per minute
λ	Excess air coefficient
CAD	Crank angle degree
IVO	Intake valve open
IVC	Intake valve close
EVO	Exhaust valve open
EVC	Exhaust valve close
fps	Frames per second
HRR	Heat release rate
IMEP	Indicated mean effective pressure
ITE	Indicated thermal efficiency
MBT	Spark timing for the maximum IMEP
ITE_{MBT}	Maximum ITE at MBT
ST	Spark timing
CA05	Crank angle when 5% mass fraction is burned
CA10	Crank angle when 10% mass fraction is burned
CA90	Crank angle when 90% mass fraction is burned
P_{max}	The maximum pressure
CA_{Pmax}	Crank angle of P_{max}
LBV	Laminar burning velocity

Introduction

With increasing concerns about environmental pollution and petroleum shortage, many multinational groups have put forward reports of policies dealing with reducing carbon footprints and moving towards carbon neutrality [1]. Considering the carbon-free policies and the huge carbon emissions from the transportation sector, the use of low-/zero-carbon fuels is the key to being carbon-neutral [2]. Compared to traditional fuels such as gasoline, natural gas (NG) has a lower carbon-to-hydrogen ratio (below 30% than gasoline). Spark-ignited (SI) engines fueled with natural gas can run at a high compression ratio or high boosting levels to obtain higher thermal efficiency thus lowering fuel consumption and carbon emission [3]. However, the poor lean-burn performance of NG results in large cycle-by-cycle variations [4], which need to be studied further.

Methane is the main ingredient of natural gas, and extensive investigations have been carried out to explore approaches for improving its lean combustion [5–7]. These investigations can be generally categorized into four categories: (1) high compression ratio or high boosting: high temperature and pressure can help improve methane lean combustion; (2) in-cylinder flow: tumble inlet ports can help increase the turbulence intensity thus flame speed; (3) ignition system: multipoint ignition can help increase the initial area of flame kernels thus the early stages of combustion can be improved; (4) dual-fuel system: highly active fuel addition can help improve methane lean combustion. For example, Fu et al. [8] found that high compression ratio can improve the thermal efficiency of methane lean combustion, and the main reason is attributed to the reduced ignition delay period; Late high-pressure direct injection is found effective to increase the turbulence intensity and thus the flame speed [9,10]; The advantages of high energy ignition [11] or double-spark ignition [12] on methane lean combustion are also confirmed recently. The above studies have clearly revealed the strategies for improving NG lean combustion in many aspects.

Among the above investigations, the addition of highly active fuel (heavy hydrocarbons/gasoline or gaseous fuels/hydrogen) gets the most attention [13–15]. Because of the zero-carbon emission and the fast flame speed, hydrogen addition has become a hot research topic, getting more and more recognition and attraction [16]. Based on a single-cylinder SI engine, Di Iorio et al. [17] and Catapano et al. [18] investigated the effects of hydrogen addition on methane combustion, and the obvious increase in thermal efficiency is ascribed to the improvement of flame speed. As for combining hydrogen addition with high compression ratio, Hora [19] studied the effect of compression ratio on hydrogen-enriched natural gas (HCNG) engine, and the results show that high compression ratio can greatly improve HCNG engine performance. Recently, Moreno et al. [20] and Reyes et al. [21] found that there exists a suitable hydrogen fraction for the natural gas/hydrogen engine, beyond or below which the engine performance will be degraded. The above studies have clearly revealed the advantages of improving NG lean combustion by hydrogen addition. However, the mechanism of methane flame characteristics with hydrogen addition is not fully understood, especially under different hydrogen injection timing and equivalence ratios.

With the above considerations, the objective of the current work is to clarify the role of hydrogen addition on methane lean combustion, with addressing hydrogen injection timings. A strengthened optical engine equipped with dual gas fuel system was adopted, and flame characteristics were addressed using high-speed direct photography. This paper is organized as follows: Experimental apparatus and analysis approach section describes the experimental apparatus and analysis approach. Results and discussion section presents a detailed comparison of methane lean combustion with addressing the hydrogen injection timing and equivalence ratios; finally, the main conclusions of the study are presented in Conclusions section.

Experimental apparatus and analysis approach

Test engine

In the current study, a single optical engine was developed in the State Key Laboratory of Engines. The engine was modified from a four-cylinder 2.0T engine, and the original pent-roof cylinder head, fuel injection system, intake/exhaust system (valve timing), ignition system were kept the same. Finally, a cylinder of 88 mm in the bore and 105 mm in stroke was obtained, ensuring a large displacement of 0.64 L. As for the other equipment, a direct current dynamometer was used for keeping the engine speed constant at 800 RPM. The excess air coefficient (λ) was measured by a wideband lambda sensor with a measurement accuracy of ±0.1%. The intake temperature was chosen for 25 ± 3 °C and atmospheric backpressure

Please cite this article as: Chen L et al., Effect of hydrogen direct injection on natural gas/hydrogen engine performance under high compression-ratio conditions, International Journal of Hydrogen Energy, https://doi.org/10.1016/j.ijhydene.2022.07.176

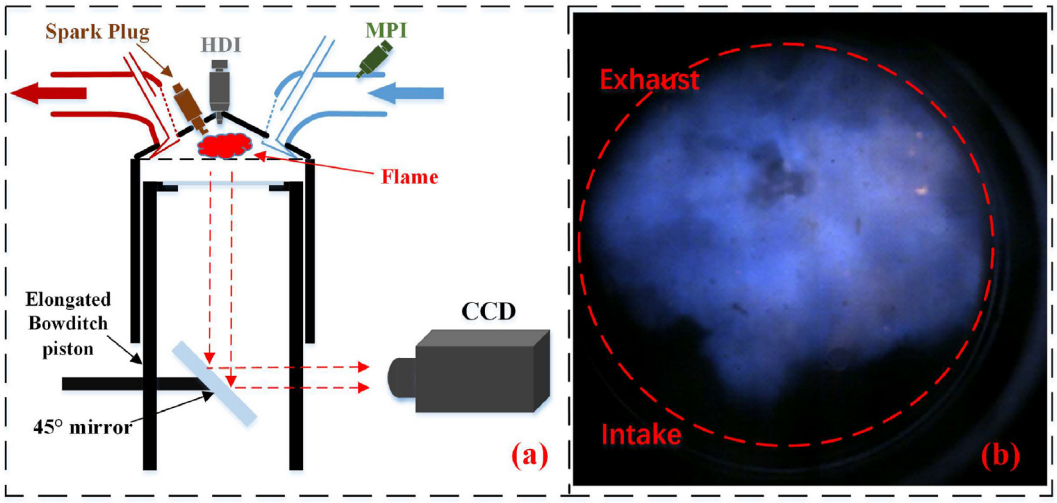

Fig. 1 – (a) Schematic of the optical measurements, (b) Direct photography result of flame image.

Table 1 – Engine specification.

Engine parameter	Value
Bore × stroke	88 × 105 mm
Sweep volume	640 cm^3
Connecting rod length	185 mm
Compression ratio	13:1
Engine speed	800 RPM
Direct injection pressure	10 MPa
Intake timing (IVO/IVC)	−330/−120 CAD
Exhaust timing (EVO/EVC)	125/340 CAD

was used irrespective of the intake pressure. The pressure was measured using a flush-installed piezo-electric transducer (Kistler 6125A), with a resolution of 0.1 crank angle degrees (CAD). Besides based on the elongated detachable piston (Fig. 1a), a high compression ratio of 13.0 was chosen for the current study. Table 1 shows the detailed parameters.

Optical measurements

Based on the elongated Bowditch piston design, an enhanced 45-degree mirror can be installed to change the combustion flame light path. The optical access to the combustion

Table 2 – Resolution or uncertainties of measured parameters and calculated values.

Parameters	Resolution/uncertainty
Engine speed	0.2%
Crank angle	0.1 CAD
Temperature	3 °C
Excess air coefficient	0.001
Cylinder pressure	1.5%
Blend ratio	0.5%
Flame image	1 pixel (0.12 mm)
Flame area at CA50	<5% (50 cycles)

Table 3 – Chemical and physical property of methane and hydrogen.

Fuel category	Methane	Hydrogen
Formula	CH_4	H_2
H/C ratio	4.0	+∞
Boiling point (°C)	−161.4	−252.77
Lower heating value (MJ/kg)	50	119.64
AI temperature [°C]	600	645
Research octane number	>120	130
Stoichiometric air-fuel ratio	17.16	34.32

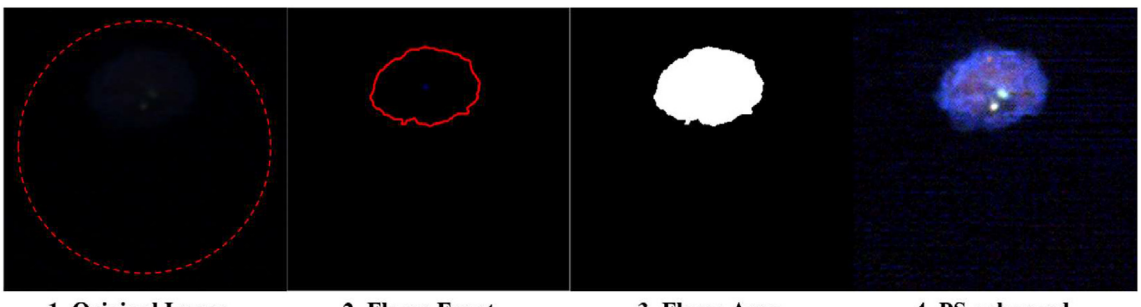

Fig. 2 – The definition of binary image and flame area.

Please cite this article as: Chen L et al., Effect of hydrogen direct injection on natural gas/hydrogen engine performance under high compression-ratio conditions, International Journal of Hydrogen Energy, https://doi.org/10.1016/j.ijhydene.2022.07.176

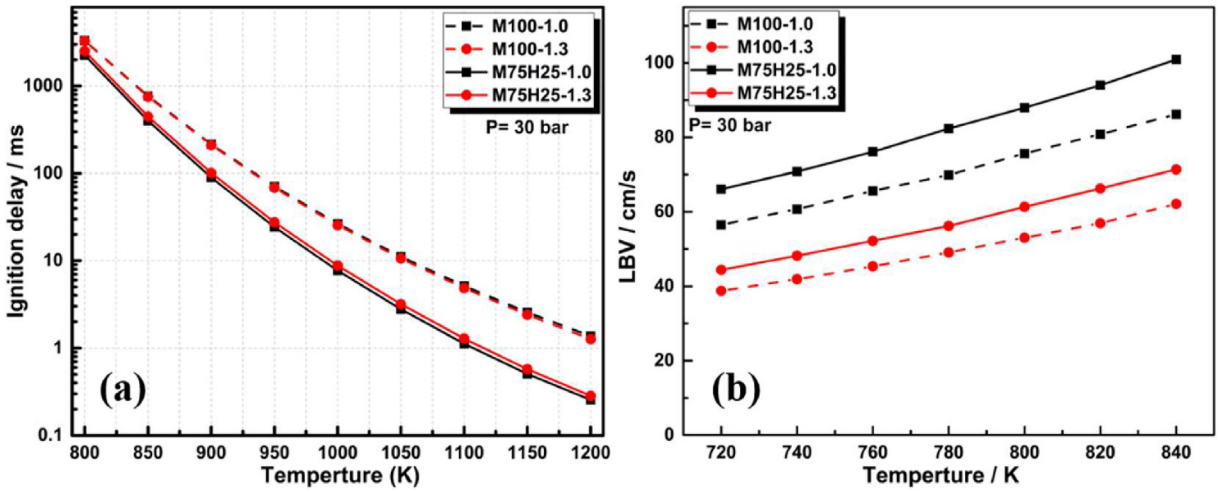

Fig. 3 – Calculated (a) ignition delay and (b) laminar burning velocity.

chamber can be found in Fig. 1a, and a high-speed camera was used to record the optical information. Although the radius (R) of the combustion chamber is 44 mm, the radius of the optical window is 31 mm due to the manufacturing constraints, accounting for 70%-cylinder radius. As shown in Fig. 1b, the flame image is provided here as an example of direct chemiluminescence, without any assistance from laser or external light source. It can be observed that the image covers the spark and injector region, and the early flame propagation is included in the optical window. Considering the temporal and spatial resolution, the camera frame rate was chosen as 9600 fps (0.5 CAD at 800 RPM) with a resolution of 512 × 512 pixels. Besides, an optical encoder was used for the synchronization of various control triggers for pressure and flame image, and 50 consecutive cycles were recorded and stored for each case.

Data analysis

For flame image analysis: macroscopic parameters related to flame morphology were estimated based on the spherical flame assumption [22,23]. Firstly, the two-dimensional projected contours of spherical flames were digitized as a matrix; then, a "binarizing–thresholding" technique was applied for the binarization. Finally, the flame contour was created and the flame area was measured. The threshold for the binarization is chosen based on the OSTU method [24]. For lean combustion, the contrast ratio of images was enhanced in Photoshop for a better direct observation. The details about the definitions of binary image and flame area are shown in Fig. 2 (M75H25, λ = 1.2, SOI = −240 CAD).

For pressure analysis: First, pressures were averaged and lightly smoothed based on five-data points weighted smoothing and 50 consecutive cycles. Second, the heat release rate (HRR) was calculated based on the first law of

Table 4 – Thermodynamic data of the two selected cases.

Case	MBT /bTDC	P_{max} /MPa	CA_{Pmax} /CAD	ST-CA5 /CAD	CA10-90 /CAD
λ = 1.0	14 CAD	4.90	15.6	13.0	21.5
λ = 1.3	22 CAD	4.02	13.4	18.6	29.0

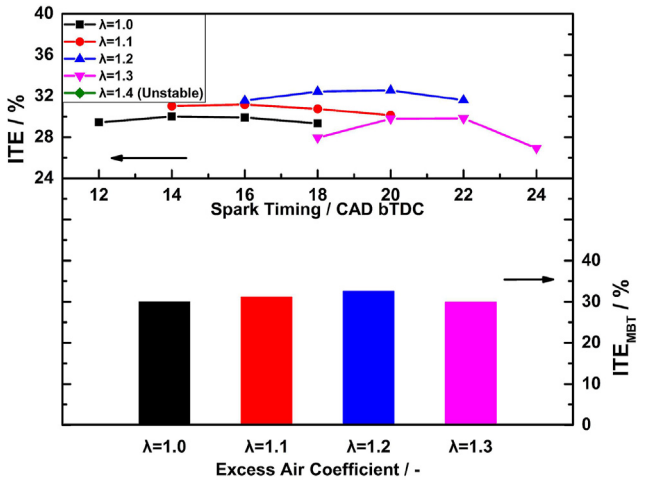

Fig. 4 – Indicated thermal efficiency of M100 at different excess air coefficients.

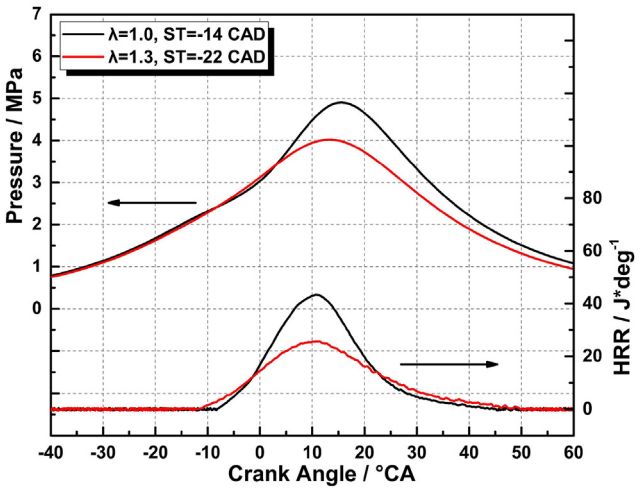

Fig. 5 – In-cylinder pressure traces and heat release rate for selected cases.

Please cite this article as: Chen L et al., Effect of hydrogen direct injection on natural gas/hydrogen engine performance under high compression-ratio conditions, International Journal of Hydrogen Energy, https://doi.org/10.1016/j.ijhydene.2022.07.176

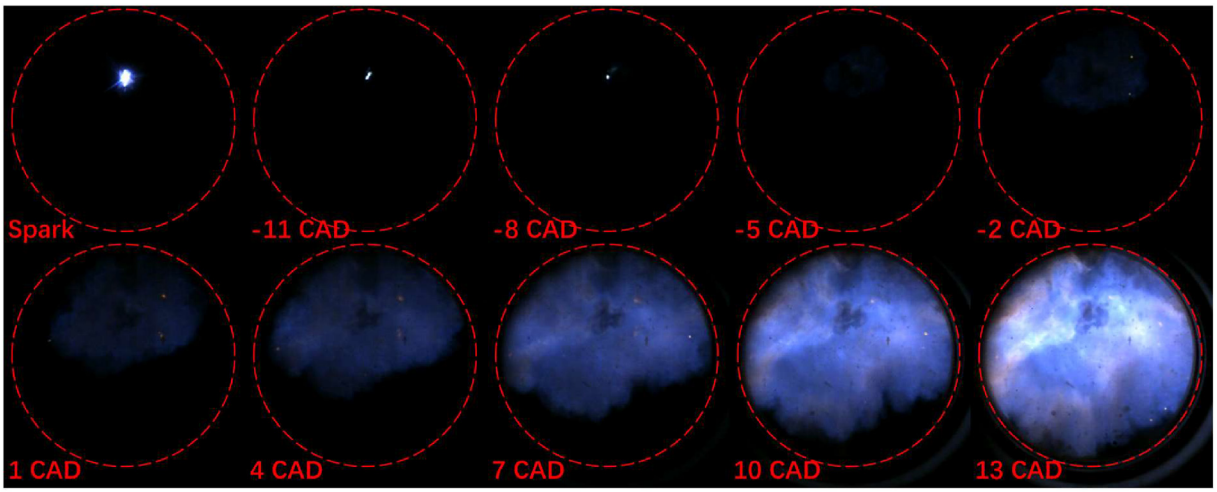

Fig. 6 – Flame images for M100 under λ = 1.0 conditions (original).

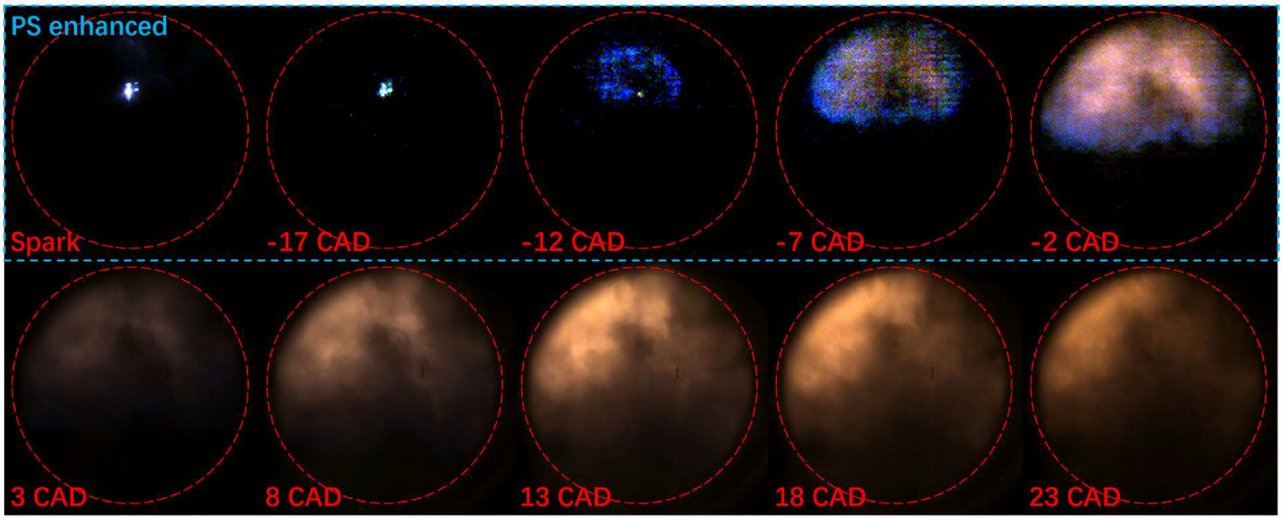

Fig. 7 – Flame images for M100 under λ = 1.3 conditions.

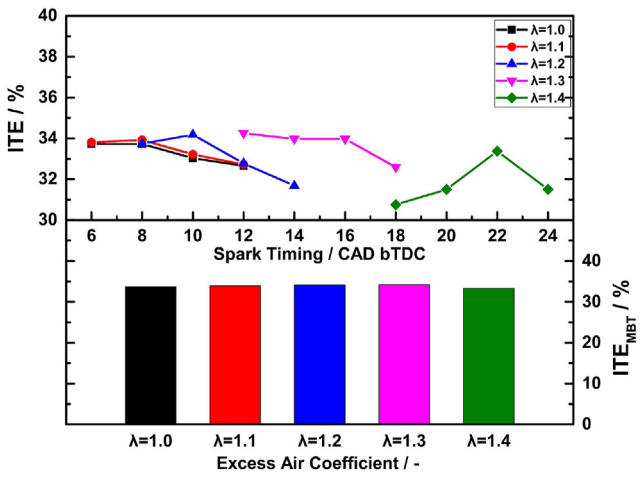

Fig. 8 – Indicated thermal efficiency of M75H25 at different excess air coefficients.

thermodynamics and a standard single-zone model. Then, the indicated mean effective pressure (IMEP) and the combustion phasing were obtained for each case [25]. Finally, the indicated thermal efficiency (ITE), which means the conversion efficiency of fuel energy to IMEP, was calculated. During the study, the uncertainties are presented in Table 2.

Fuel property

As shown in Fig. 1a, a dual-fuel supply system including port and direct injectors was used in this study, and the fuel used

Table 5 – Thermodynamic data of the three selected cases.

Case	MBT /bTDC	P_{max} /MPa	CA_{Pmax} /CAD	ST-CA5 /CAD	CA10-90 /CAD
λ = 1.0	8 CAD	4.38	17.9	9.8	20.3
λ = 1.2	10 CAD	4.18	16.6	11.0	22.1
λ = 1.4	22 CAD	3.89	10.4	16.6	32.7

Please cite this article as: Chen L et al., Effect of hydrogen direct injection on natural gas/hydrogen engine performance under high compression-ratio conditions, International Journal of Hydrogen Energy, https://doi.org/10.1016/j.ijhydene.2022.07.176

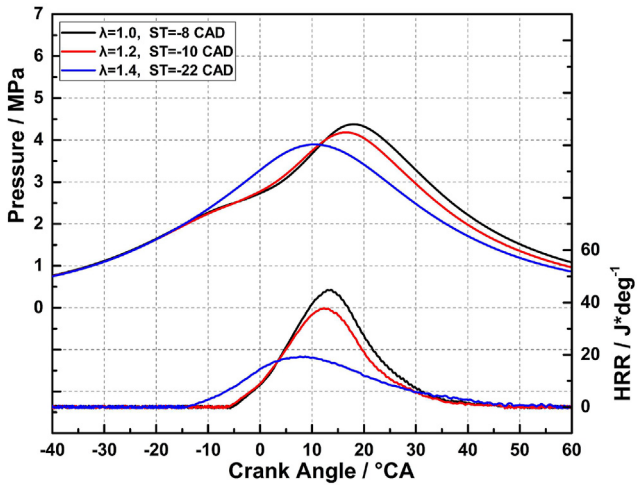

Fig. 9 – In-cylinder pressure traces and heat release rate for selected cases.

in the experiment was methane (port injection) and hydrogen (direct injection). The direct injector is a six-hole injector and mounted vertically in the center of cylinder head. For a better homogeneity, a high injection pressure of 10 MPa is chosen. The fuel properties of methane and hydrogen were shown in Table 3. Before the study, the author consulted the reference about HCNG combustion and found that 20–30% by mole is a suitable hydrogen fraction for the natural gas/hydrogen engine considering both engine efficiency and knock tendency [20,21]. Thus, a fixed ratio (25% by mole, M75H25) was chosen in the current study. Based on a zero-dimensional simulation (Chemkin-Pro 18.0) and GRI 3.0 chemical mechanisms, the ignition delay time and laminar burning velocity (LBV) of M75H25 are illustrated in Fig. 3. Hydrogen addition can result in high chemical reactivity, consequently promoting the burning rate and flame propagation. It is observed that hydrogen addition can greatly decrease the ignition delay and increase the LBV of methane. In the next section, the influences of hydrogen on methane combustion and cyclic variation are discussed based on M75H25.

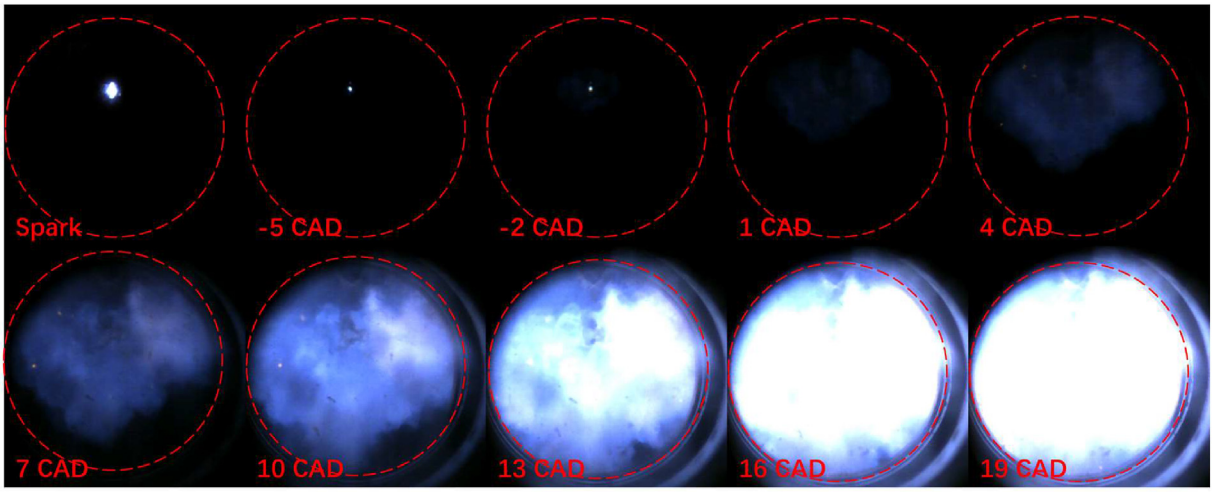

Fig. 10 – Flame images for M75H25 under λ = 1.0 conditions (original).

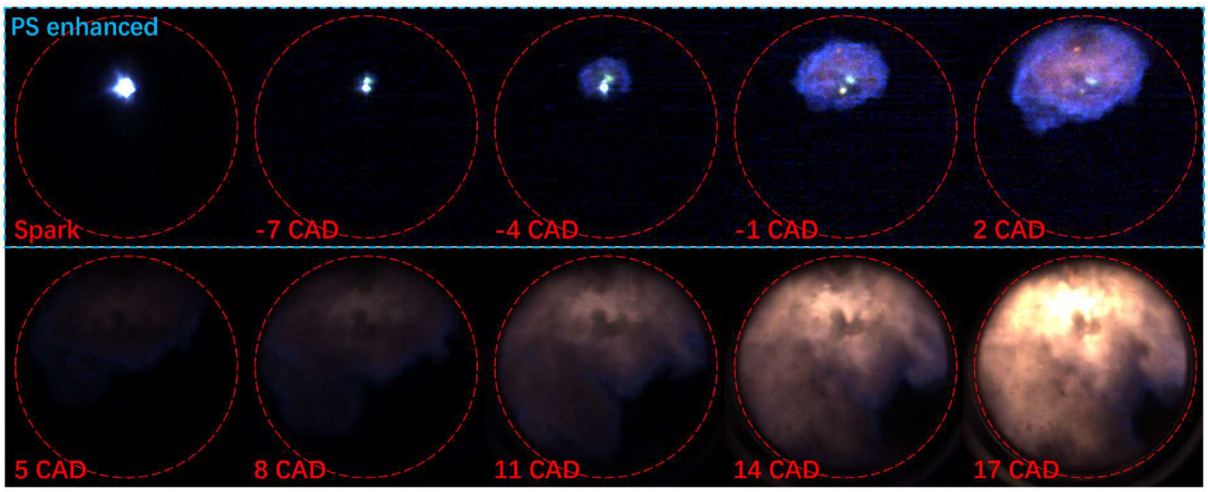

Fig. 11 – Flame images for M75H25 under λ = 1.2 conditions.

Please cite this article as: Chen L et al., Effect of hydrogen direct injection on natural gas/hydrogen engine performance under high compression-ratio conditions, International Journal of Hydrogen Energy, https://doi.org/10.1016/j.ijhydene.2022.07.176

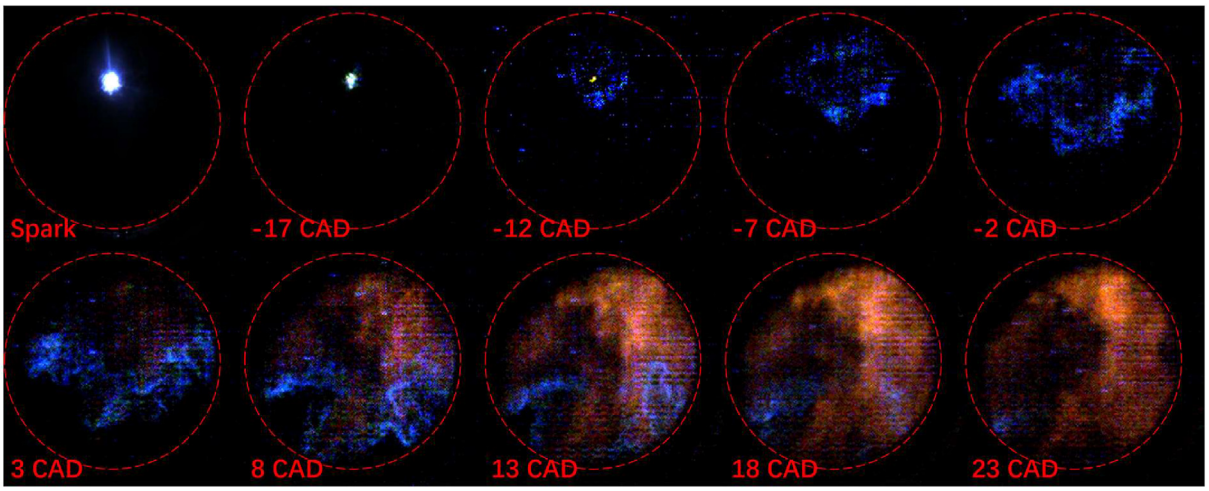

Fig. 12 – Flame images for M75H25 under λ = 1.4 conditions (PS enhanced).

Results and discussion

Methane combustion with hydrogen additions

Based on pure methane (M100), SI combustion under different lean conditions was studied first, and the engine combustion performance was represented by the indicated thermal efficiency. Fig. 4 shows the ITE versus spark timing at different excess air coefficients (λ) and the maximum ITE (ITE_{MBT}) is shown at the bottom. It can be observed that lean combustion can improve engine's thermal efficiency, and the peak ITE is about 32.5% at ST = −20 CAD under λ = 1.2 conditions. However, there is a trend that ITE decreases with further increasing excess air coefficient, which is due to the higher cycle-to-cycle variation under λ = 1.3 conditions [26]. More to the point, under λ = 1.4 conditions, the lean-burn performance of methane is too poor, so stable combustion cannot be achieved.

For a complete understanding of the combustion characteristic under stoichiometric and lean conditions, two cases (λ = 1.0 and 1.3) were selected and the related thermodynamic details are listed in Table 4. Fig. 5 shows the in-cylinder pressure traces and the corresponding heat release rates. Since the MBT is chosen, it can be observed that both the combustions are around the optimum combustion phase. The peak pressure of λ = 1.0 is 4.90 MPa at 15.6 CAD and that of λ = 1.3 is 4.02 MPa at 13.4 CAD. Under lean conditions, the initial flame formation (ST-CA05) but also the fast turbulent flame propagation (CA10-90) are longer, which is the main reason for the combustion cycle-to-cycle variations [22].

From pressure signal analysis it was not possible to obtain further details about the evolution of the combustion phenomena that occurred in the combustion chamber, Figs. 6 and 7 show the corresponding flame images. The cycles of the flame images are chosen according to the average pressure (Fig. 5). As shown in the picture, the starting image is chosen as the spark timing and the flame front was initiated in the spark plug region. Then, the flame front expanded around until reaching the optical limit. For stoichiometric combustion (Fig. 6), the original flame is bright and blue, which is due to CH* under high-temperature combustion conditions. For lean combustion (Fig. 7), the flame is not bright enough in the early stage. After 3 CAD, the original flame is yellow, which is due to C* under low-temperature combustion conditions. Besides, the combustion ratio is obviously lower under lean conditions.

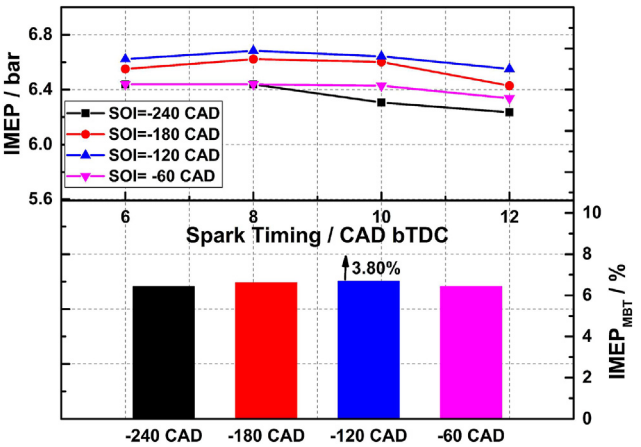

Fig. 13 – IMEP of M75H25 under four injection timings and λ = 1.0 conditions.

As discussed above, lean combustion can improve methane engine's thermal efficiency. However, there exists a lean limit and the combustion even becomes unstable at a high excess air coefficient (λ = 1.4), which is due to the poor combustion performance under lean conditions. In this section, the effect of hydrogen addition on methane lean combustion was explored and the injection timing is fixed at −240 CAD for a homogeneous mixture. Fig. 8 shows the indicated thermal efficiency of M75H25 versus spark timing at different

Table 6 – Thermodynamic data of the four selected cases.

SOI	P_{max}	CA_{Pmax}	ST-CA05	CA10-CA90
−240 CAD	4.82 MPa	15.5 CAD	10.0 CAD	20.8 CAD
−180 CAD	4.97 MPa	15.3 CAD	9.5 CAD	20.0 CAD
−120 CAD	5.13 MPa	14.9 CAD	9.2 CAD	19.6 CAD
−60 CAD	5.59 MPa	12.5 CAD	8.0 CAD	17.2 CAD

Please cite this article as: Chen L et al., Effect of hydrogen direct injection on natural gas/hydrogen engine performance under high compression-ratio conditions, International Journal of Hydrogen Energy, https://doi.org/10.1016/j.ijhydene.2022.07.176

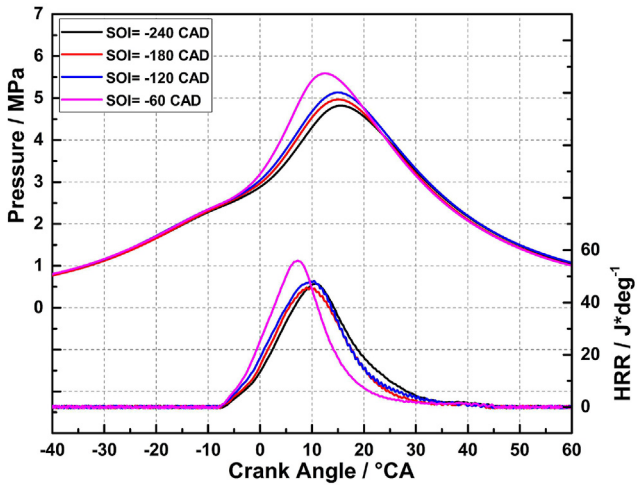

Fig. 14 – In-cylinder pressure traces and heat release rate for selected cases.

excess air coefficients. Similar to M100, lean combustion can also improve the thermal efficiency of M75H25. The trend (ITE increases first and then decreases with excess air coefficient) is also the same as that of M100, however, the difference is little under different excess air coefficient conditions when comparing the ITE_{MBT}. When comparing M75H25 to M100, hydrogen addition can greatly improve the indicated thermal efficiency and the peak ITE is about 34.3% at ST = −12 CAD under $\lambda = 1.3$ conditions. Besides, the turning point of M75H25 locates at $\lambda = 1.3$, and stable combustion is achieved under $\lambda = 1.4$ conditions. This phenomenon means hydrogen addition not only improves thermal efficiency of methane combustion, but also the combustion stability.

Three cases ($\lambda = 1.0$, 1.2 and 1.4) were selected and the related thermodynamic details are listed in Table 5. Fig. 9 shows the effect of excess air coefficient (λ) on pressure and corresponding heat release rate, and the spark timing is chosen as MBT. It can be seen that excess air coefficient has a great influence on M75H25 combustion phase under the current condition. With the increase of excess air coefficient, the MBT is significantly advanced. While comparing the cases to M100, different combustion behaviors were noted. For $\lambda = 1.0$, the initial flame formation (ST-CA05) of M75H25 is about 9.8 CAD and that of M100 is 13.0, besides, the flame propagation (CA10-90) is also shorter. Under lean conditions, the ST-CA05 of M75H25 at $\lambda = 1.4$ is shorter than that of M100 at $\lambda = 1.3$ ($16.6 < 18.6$), the CA10-90 of M75H25 at $\lambda = 1.4$ is longer than that of M100 at $\lambda = 1.3$ ($32.7 > 29.0$). This phenomenon means that hydrogen addition mainly acts as an ignition promoter for methane lean combustion.

Figs. 10–12 show the corresponding flame images of the selected cases of M75H25. The three cycles (the flame images) are chosen according to the average pressure (Fig. 9). As shown in the picture, the starting image is chosen as the spark timing and the flame front was initiated in the spark plug region. Then, the spark-induced flame propagates to the surrounding with a stretched and wrinkled front. For stoichiometric combustion (Fig. 10), the flame is bluer and brighter, and almost fully occupies the cylinder with a duration of 21 CAD. For lean combustion of $\lambda = 1.2$ (Fig. 11), the flame is not bright enough in the early stage, and the duration of flame propagation is about 27 CAD. When further increasing the excess air coefficient ($\lambda = 1.4$ in Fig. 12), the flame of the whole stage is not bright enough, and the whole duration is also the longest (40 CAD).

Stoichiometric combustion of M75H25 at different injecting timings

Thanks to the dual-fuel supply system, the effect of hydrogen injection timings on methane combustion is discussed in this section. As discussed in Methane combustion with hydrogen

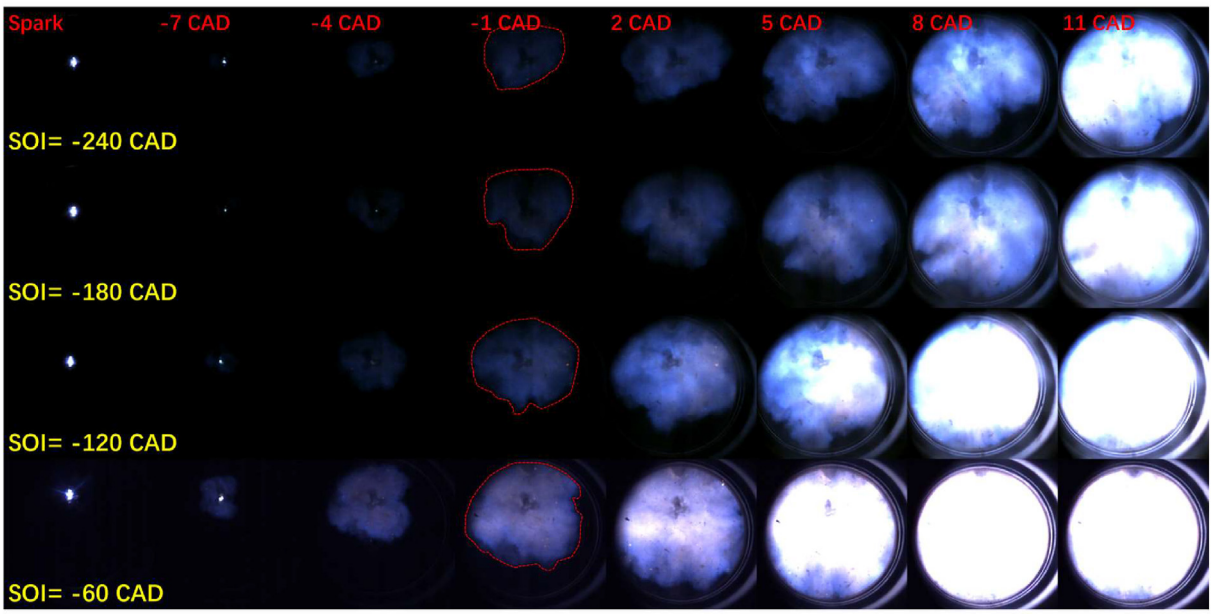

Fig. 15 – Flame images under four injection timings and $\lambda = 1.0$ conditions (original).

Please cite this article as: Chen L et al., Effect of hydrogen direct injection on natural gas/hydrogen engine performance under high compression-ratio conditions, International Journal of Hydrogen Energy, https://doi.org/10.1016/j.ijhydene.2022.07.176

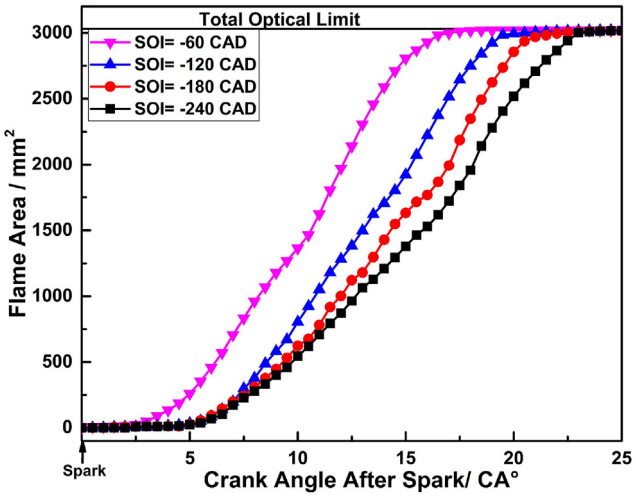

Fig. 16 – Flame areas under four injection timings and λ = 1.0 conditions.

additions section, the flame is not bright enough to be observed under λ = 1.3 and 1.4 conditions, so the study of injection timing is based on λ = 1.0 (stoichiometric condition) and λ = 1.2 (lean condition). Based on the stoichiometric condition, Fig. 13 shows the IMEP versus spark timing at different injection timing and the engine performance was represented by the IMEP. It can be observed that late hydrogen injection can improve M75H25 engine performance. The peak IMEP (6.68 bar) is obtained at SOI = −120 CAD and ST = −8 CAD, and the increment is 3.80%. Usually, late injection can increase the turbulence intensity (flame speed) inside the cylinder, as a result, the engine performance can be improved [27]. However, there is a trend that IMEP decreases with further delayed injection timing. For SOI = −60 CAD, the engine performance is lowered, located between the cases of SOI = −240 CAD and SOI = −180 CAD. The possible reason is that the mixture (hydrogen) of SOI = −120 CAD is inhomogeneous and the thermal efficiency is decreased. This phenomenon means that there exists a compromise for turbulence intensity and inhomogeneity if late injection is adopted.

Table 7 – Thermodynamic data of selected cycles.

SOI	P_{max}	CA_{Pmax}	ST-CA05	CA10-CA90
−240 CAD	4.18 MPa	16.6 CAD	11.0 CAD	22.1 CAD
−180 CAD	4.32 MPa	16.5 CAD	10.6 CAD	21.6 CAD
−120 CAD	4.42 MPa	16.0 CAD	10.4 CAD	21.0 CAD
−60 CAD	4.92 MPa	13.9 CAD	8.9 CAD	18.2 CAD

For a complete understanding of the combustion characteristic under different injection timing conditions, four cases were selected and the related thermodynamic details are listed in Table 6. Fig. 14 shows the in-cylinder pressure and the corresponding HRR at different injection timings, and the spark timing is chosen as −10 CAD. As shown in Fig. 14, the in-cylinder pressure is significantly affected by the injection timing. At the earliest injection timing of −240 CAD, there is a relatively gentle slope in the pressure graph and the peak pressure is about 4.82 MPa at 15.5 CAD. As the injection timing is retarded (from −240 CAD to −120 CAD), the combustion rate is a little increased. For SOI = −60 CAD, the pressure increases steeply and reaches the maximum of 5.59 MPa at 12.5 CAD. As for HRR, the fastest combustion is observed at the latest injection timing of −60 CAD, manifesting a fast initial flame formation (ST-CA05) and turbulent flame propagation (CA10-90).

Based on the average pressure, Fig. 15 shows the original flame images of the four chosen cycles. For SOI = −240 CAD, as shown in the upper of Fig. 15, there is a spark-induced light when the spark ignition happened. After the spark, the flame front propagates to the surrounding and the behavior is nearly the same as that in Fig. 10. When the SOI is delayed, the flame area is increased (as shown by the red circle), which means a higher flame speed. The fastest flame speed is observed under SOI = −60 CAD conditions. Usually, the propagation direction is nearly the same (upper left, high temperature), and the region of unburned mixture locates at the bottom right corner (−240 CAD). However, the flame front propagation is changed with the injection timing, manifesting by the different locations of the unburned mixture. The main reason is the different turbulence flow induced by different injection timings. Fig. 16 shows a more intuitive display of the flame area. It

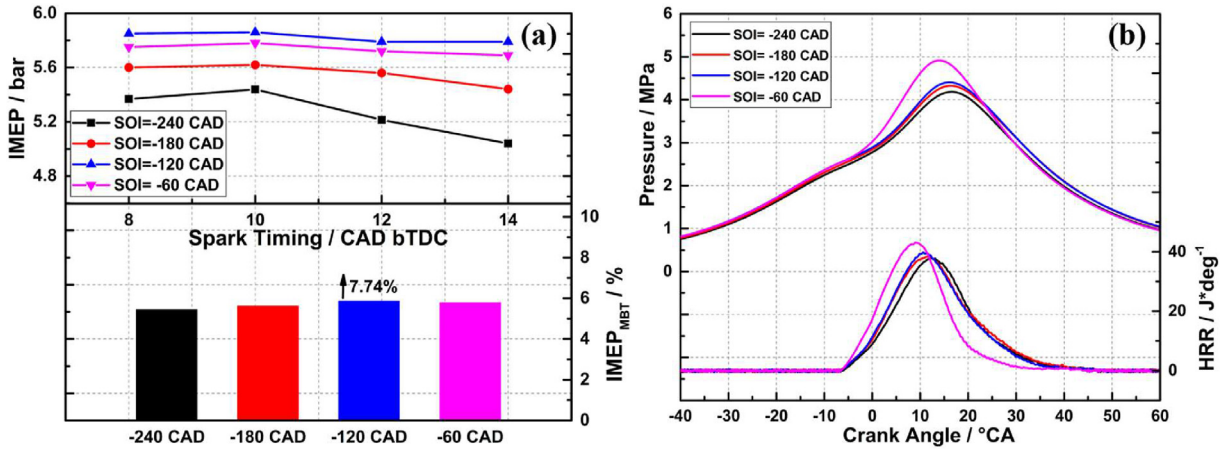

Fig. 17 – (a) IMEP (b) In-cylinder pressure traces and heat release rate under four injection timings and λ = 1.2 conditions.

Please cite this article as: Chen L et al., Effect of hydrogen direct injection on natural gas/hydrogen engine performance under high compression-ratio conditions, International Journal of Hydrogen Energy, https://doi.org/10.1016/j.ijhydene.2022.07.176

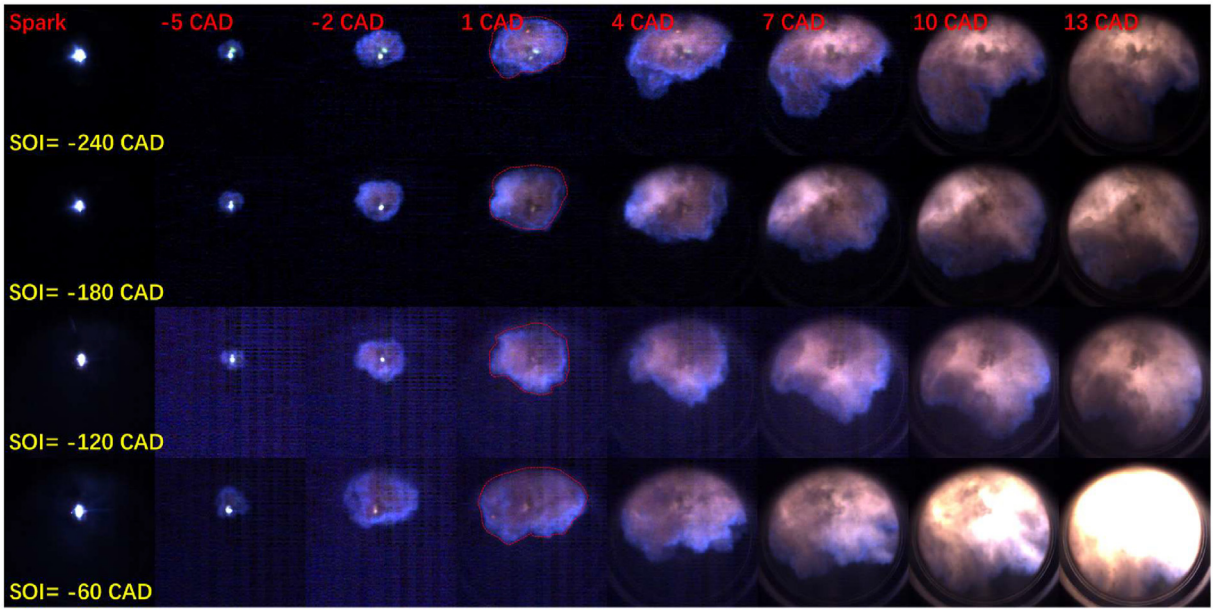

Fig. 18 – Flame images under four injection timings and λ = 1.2 conditions (PS enhanced).

can be observed that late injection can greatly promote flame propagation, especially for −60 CAD case. Through the whole combustion phase, the flame area of −60 CAD is nearly 2 times that of −240 CAD, which is consistent with the trend of the combustion phase in Table 6.

Lean combustion of M75H25 at different injecting timings

Based on lean condition (λ = 1.2), Fig. 17a shows the IMEP versus spark timing at different injection timing. Similar to the stoichiometric condition, late hydrogen injection can also improve M75H25 lean combustion. The peak IMEP (5.86 bar) is obtained at SOI = −120 CAD and ST = −10 CAD, with an increment of 7.74%. Besides, IMEP also decreases with further delayed injection timing. However, the improvement is higher than that of Fig. 13, and the IMEP of SOI = −60 CAD locates between the cases of SOI = −120 CAD and SOI = −180 CAD. The difference may due to that the inhomogeneity is reduced under lean conditions (less mass of hydrogen). Fig. 17b shows the in-cylinder pressure and the corresponding HRR of ST = −10 CAD, the related thermodynamic details are listed in Table 7. As shown in Fig. 17b, the trend of in-cylinder pressure is also similar to that of stoichiometric condition, the combustion phase is advanced with the delay of the injection timing, and the fastest combustion is also observed at the latest injection timing of −60 CAD.

Fig. 18 shows the flame images (PS enhanced image, except for spark) of the four chosen cycles under lean conditions. It is observed that the brightness of the four spark lights is nearly the same under the current condition. After the spark, the spark-induced flame propagates to the surrounding with a stretched and wrinkled front. When the SOI is delayed, the flame area is increased (as shown by the red circle), which means a higher flame speed. Besides for SOI = −60 CAD, the flame almost fully occupies the cylinder at 10 CAD with a duration of 20 CAD, and the flame is also bright with white

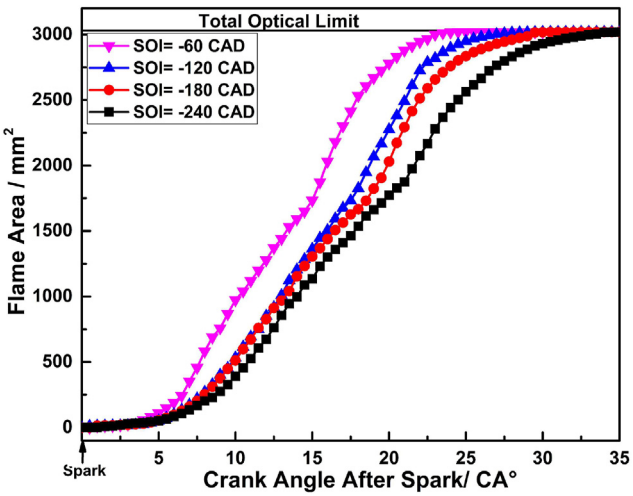

Fig. 19 – Flame area under four injection timings and λ = 1.2 conditions.

light. Fig. 19 shows a more intuitive display of the flame area under the current lean conditions. It can be observed that late hydrogen injection can greatly promote methane lean combustion. In the early stages of methane combustion (from spark to −5 CAD), the initial flame area is nearly the same from −240 CAD to −60 CAD. However, the subsequent upward trend is much bigger when the injection timing is −60 CAD, which is consistent with the data in Table 7.

Conclusions

To experimentally clarify the effect of hydrogen addition and direct injection timing on methane lean combustion, an optical engine equipped with a dual-fuel supply system was

Please cite this article as: Chen L et al., Effect of hydrogen direct injection on natural gas/hydrogen engine performance under high compression-ratio conditions, International Journal of Hydrogen Energy, https://doi.org/10.1016/j.ijhydene.2022.07.176

adopted. The blended ratio of hydrogen was chosen as 25% (by mole) and the injection timing was varied from −240 CAD to −60 CAD. Flame propagation (especially the early flame) was addressed using high-speed direct photography, and simultaneous pressure acquisition was also applied for analyzing engine performance. The following conclusions can be drawn.

1. Lean combustion can improve the methane engine's thermal efficiency; however, thermal efficiency will decrease if the excess air coefficient is too high (≥1.3). Besides, the flame of methane stoichiometric combustion is blue (CH*), while the flame of methane lean combustion is yellow (C*).
2. Hydrogen addition mainly acts as an ignition promoter for methane lean combustion, as a result, the poor lean-burn performance of methane can be greatly improved. 25% hydrogen addition can increase the thermal efficiency of methane combustion, but also can extend the lean combustion limit.
3. Late hydrogen injection can increase the in-cylinder turbulence intensity but also the mixture inhomogeneity, there exists a compromise if a late injection is adopted. So, a suitable hydrogen injection timing is needed for improving the methane/hydrogen engine's performance.
4. For improving methane/hydrogen engine's performance, late hydrogen injection is more effective under lean conditions. The main reason is that the mixture inhomogeneity is reduced under lean conditions.

In summary, this work optically evaluated the effect of hydrogen injection timing on methane combustion under different equivalence ratio conditions. It can give some insights into the controlling strategies when natural gas/hydrogen engines operate in dual-injection mode. Future work will focus on examining the knocking characteristic under high boosting conditions.

Declaration of competing interest

The authors declare that they have no known competing financial interests or personal relationships that could have appeared to influence the work reported in this paper.

Acknowledgements

This study was supported by National Natural Science Foundation of China (52076149, 51825603) and Educational Commission of Hubei Province of China (Q20211509).

REFERENCES

[1] Karimi M, Wang X, Hamilton J, Negnevitsky M, Lyden S. Status, challenges and opportunities of dual fuel hybrid approaches-a review. Int J Hydrogen Energy 2021;46:34924–57.
[2] Hall C, Kassa M. Advances in combustion control for natural gas-diesel dual fuel compression ignition engines in automotive applications: a review. Renew Sustain Energy Rev 2021;148:111291.
[3] Lee J, Park C, Bae J, Kim Y, Lee S, Kim C. Comparison between gasoline direct injection and compressed natural gas port fuel injection under maximum load condition. Energy 2020;197:117173.
[4] Boulahlib MS, Medaerts F, Boukhalfa MA. Experimental study of combustion performances and emissions of a spark ignition cogeneration engine operating in lean conditions using different fuels. Int J Hydrogen Energy 2018;43:3586–96.
[5] Ma F, Ding S, Wang Y, Wang Y, Wang J, Zhao S. Study on combustion behaviors and cycle-by-cycle variations in a turbocharged lean burn natural gas S.I. engine with hydrogen enrichment. Int J Hydrogen Energy 2008;33:7245–55.
[6] Korakianitis T, Namasivayam A, Crookes R. Natural-gas fueled spark-ignition (SI) and compression-ignition (CI) engine performance and emissions. Prog Energy Combust Sci 2011;37:89–112.
[7] Li M, Wu H, Zhang T, Shen B, Zhang Q, Li Z. A comprehensive review of pilot ignited high pressure direct injection natural gas engines: factors affecting combustion, emissions and performance. Renew Sustain Energy Rev 2020;119:109653.
[8] Fu J, Shu J, Zhou F, Liu J, Xu Z, Zeng D. Experimental investigation on the effects of compression ratio on in cylinder combustion process and performance improvement of liquefied methane engine. Appl Therm Eng 2017;113:1208–18.
[9] Song J, Park S. Combustion characteristics of a methane engine with Air- and N-2-assisted direct injection. Fuel 2017;209:350–7.
[10] Song J, Choi M, Kim D, Park S. Combustion characteristics of methane direct injection engine under various injection timings and injection pressures. J Eng Gas Turbines Power-Trans ASME 2017;139:82802.
[11] Chen L, Wei H, Zhang R, Pan J, Zhou L, Feng D. Effects of spark plug type and ignition energy on combustion performance in an optical SI engine fueled with methane. Appl Therm Eng 2019;148:188–95.
[12] Duan X, Zhang S, Liu Y, Li Y, Liu J, Lai M, Deng B. Numerical investigation the effects of the twin-spark plugs coupled with EGR on the combustion process and emissions characteristics in a lean burn natural gas SI engine. Energy 2020;206:118181.
[13] Akansua S, Dulgerb Z, Kahramana N, Veziroglu T. Internal combustion engines fueled by natural gas-hydrogen mixtures. Int J Hydrogen Energy 2004;33:1527–39.
[14] Chen H, He J, Zhong X. Engine combustion and emission fuelled with natural gas: a review. J Energy Inst 2019;92:1123–36.
[15] Chen Z, Zhang T, Wang X, Chen H, Geng L, Zhang T. A comparative study of combustion performance and emissions of dual-fuel engines fueled with natural gas/methanol and natural gas/gasoline. Energy 2021;237:121586.
[16] Alrazena H, Ahmad KA. HCNG fueled spark-ignition (SI) engine with its effects on performance and emissions. Renew Sustain Energy Rev 2018;82:324–42.
[17] Di Iorio S, Sementa P, Vaglieco BM. Analysis of combustion of methane and hydrogen-methane blends in small DI SI (direct injection spark ignition) engine using advanced diagnostics. Energy 2016;108:99–107.
[18] Catapano F, Di Iorio S, Magno A, Sementa P, Vaglieco BM. A comprehensive analysis of the effect of ethanol, methane and methane-hydrogen blend on the combustion process in a PFI (port fuel injection) engine. Energy 2015;88:101–10.
[19] Hora TS, Agarwal AK. Effect of varying compression ratio on combustion, performance, and emissions of a hydrogen enriched compressed natural gas fuelled engine. J Nat Gas Sci Eng 2016;31:819–28.

Please cite this article as: Chen L et al., Effect of hydrogen direct injection on natural gas/hydrogen engine performance under high compression-ratio conditions, International Journal of Hydrogen Energy, https://doi.org/10.1016/j.ijhydene.2022.07.176

[20] Moreno F, Muñoz M, Arroyo J, Magén O, Monné C, Suelves I. Efficiency and emissions in a vehicle spark ignition engine fueled with hydrogen and methane blends. Int J Hydrogen Energy 2012;37(15):11495–503.
[21] Reyes M, Tinaut FV, Melgar A, Perez A. Characterization of the combustion process and cycle-to-cycle variations in a spark ignition engine fuelled with natural gas/hydrogen mixtures. Int J Hydrogen Energy 2016;41(3):2064–74.
[22] Aleiferis PG, Taylor AMKP, Ishii K, Urata Y. The nature of early flame development in a lean-burn stratified-charge spark-ignition engine. Combust Flame 2004;136(3):283–302.
[23] Ma X, Wang Z, Jiang CZ, Jiang YZ, Xu HM, Wang JX. An optical study of in-cylinder CH2O and OH chemiluminescence in flame-induced reaction front propagation using high speed imaging. Fuel 2014;136:603–10.
[24] Otsu N. A threshold selection method from gray-level histograms. IEEE Trans Syst Man Cybern Syst 1979;9:62–6.
[25] Wu Y, Rossow B, Modica V, Yu XL, Wu LL, Grisch F. Laminar flame speed of lignocellulosic biomass-derived oxygenates and blends of gasoline/oxygenates. Fuel 2017;202:572–82.
[26] Gomez Montoya J, Amell A, Olsen D, Amador Diaz G. Strategies to improve the performance of a spark ignition engine using fuel blends of biogas with natural gas, propane and hydrogen. Int J Hydrogen Energy 2018;43:21592–602.
[27] Chen L, Wei H, Zhang R, Pan J, Zhou L, Liu C. Effects of late injection on lean combustion characteristics of methane in a high compression ratio optical engine. Fuel 2019;255:115718.

Please cite this article as: Chen L et al., Effect of hydrogen direct injection on natural gas/hydrogen engine performance under high compression-ratio conditions, International Journal of Hydrogen Energy, https://doi.org/10.1016/j.ijhydene.2022.07.176